



1

2                   Geophysical Research Letters

3

4                   Supporting Information for

5

6                   **Local and remote impacts of atmospheric cloud  
7                   radiative effects onto the eddy-driven jet**

8

9

10                  O. Watt-Meyer<sup>1</sup>, and D. M. W. Frierson<sup>1</sup>

11                  <sup>1</sup>Department of Atmospheric Sciences, University of Washington, Seattle, USA

12

13

14

15

16

17

18

19

20 **S1. Latitude-dependent clouds-on experiments**

21 In order to investigate the separate effects of tropical and extratropical clouds onto the  
 22 eddy-driven jet, experiments additional to the standard COOKIE procedure are  
 23 performed in which cloud radiative effects are turned on/off in only certain latitude  
 24 bands, or for only LW versus SW. A weighting function that depends on latitude is  
 25 constructed to smoothly interpolate between total radiative fluxes and heating rates,  
 26 which include cloud radiative effects, and clear-sky fluxes and heating rates, which don't.  
 27 Specifically, the weighting function is defined as

$$28 \quad w(\phi, \phi_{ET}, \Delta\phi) = \begin{cases} 1, & |\phi| \geq \phi_{ET} + \Delta\phi/2 \\ 0, & |\phi| < \phi_{ET} - \Delta\phi/2 \\ 0.5 \left(1 - \sin \left[\frac{\pi}{\Delta\phi} (\phi - \phi_{ET})\right]\right), & \phi_{ET} - \frac{\Delta\phi}{2} < \phi < \phi_{ET} + \frac{\Delta\phi}{2} \\ 0.5 \left(1 + \sin \left[\frac{\pi}{\Delta\phi} (\phi + \phi_{ET})\right]\right), & -\phi_{ET} - \frac{\Delta\phi}{2} < \phi < -\phi_{ET} + \frac{\Delta\phi}{2} \end{cases} \quad (\text{S1})$$

29 where  $\phi_{ET}$  is the boundary between clouds-on and clouds-off regions and  $\Delta\phi$  is the width  
 30 of the smoothing region between clouds off and clouds on. The weighting function  $w$  is  
 31 plotted in Fig. S1 using the parameters  $\phi_{ET} = 30^\circ$  and  $\Delta\phi = 10^\circ$ . Four experiments are  
 32 performed with the GFDL-AM2.1 model in which cloud radiative effects are only  
 33 included in certain latitude bands. These are: deep tropics (equatorward of  $15^\circ$ ), tropics  
 34 (equatorward of  $30^\circ$ ), subtropics (between  $15^\circ$  and  $30^\circ$ ) and extratropics (poleward of  
 35  $30^\circ$ ). For the NCAR-CAM5.3 model, only the tropics and extratropics experiments are  
 36 performed. Given some heating rate or radiative flux  $Q$ , which is computed by the  
 37 radiative transfer scheme for both total ( $Q_{total}$ ) and clear-sky ( $Q_{clearsky}$ ) conditions, the  
 38 actual heating rate or flux imposed in each of these simulations is given by:

39

$$40 \quad Q_{extratrop\,on} = Q_{total} \cdot (1 - w(\phi_{ET} = 30^\circ, \Delta\phi = 10^\circ)) + Q_{clearsky} \cdot w(\phi_{ET} = 30^\circ, \Delta\phi = 10^\circ) \quad (\text{S2})$$

$$41 \quad Q_{tropical\;on} = Q_{total} \cdot w(\phi_{ET} = 30^\circ, \Delta\phi = 10^\circ) + Q_{clearsky} \cdot (1 - w(\phi_{ET} = 30^\circ, \Delta\phi = 10^\circ)) \quad (S33)$$

$$42 \quad Q_{deep\ trop\ on} = Q_{total} \cdot w(\phi_{ET} = 15^\circ, \Delta\phi = 5^\circ) + Q_{clearsky} \cdot (1 - w(\phi_{ET} = 15^\circ, \Delta\phi = 5^\circ)) \quad (S4)$$

$$Q_{subtrop\;on} = Q_{total} \cdot [w(\phi_{ET} = 30^\circ, \Delta\phi = 5^\circ) - w(\phi_{ET} = 15^\circ, \Delta\phi = 5^\circ)] +$$

$$Q_{clearsky} \cdot [1 - w(\phi_{ET} = 30^\circ, \Delta\phi = 5^\circ) + w(\phi_{ET} = 15^\circ, \Delta\phi = 5^\circ)] \quad (S5)$$

44

45 In addition to the above-described experiments, two simulations are performed with the  
46 GFDL-AM2.1 model in which cloud radiative effects are included only for the longwave  
47 or shortwave bands separately.

48

49

50

51

52

53

54

55

56

57

58

59

60

61

62

63

64

65 **Tables**

66 Table S1: The values of the eddy-driven jet latitude in the clouds-off simulation, and its  
 67 shift ( $\Delta\phi$ ), the Hadley cell strength in the clouds-off simulation, and its shift ( $\Delta\psi$ ) and  
 68 ACRE\_GRAD\_diff for each supplemental experiment in which cloud radiative effects are only  
 69 imposed in certain latitude bands, or for only the LW or SW bands. The length of each  
 70 simulation is also shown.

Experiment	Region/type of cloud radiative effects	$\phi_{off}$ [°N]	$\Delta\phi$ [° pole-ward]	$\psi_{off}$ [ $10^9$ kg/s]	$\Delta\psi$ [ $10^9$ kg/s]	ACRE_GRAD_diff [ $10^{-6}$ W/m <sup>3</sup> ]	Length of run [years]
GFDL-AM2.1, extratropical on	Imposed poleward of 30°, following Eq. S2	39.7	2.27	160.4	-0.6	-7.77	60
GFDL-AM2.1, tropical on	Imposed equatorward of 30°, following Eq. S3	39.7	-1.94	160.4	37.2	0.74	60
GFDL-AM2.1, deep tropical on	Imposed equatorward of 15°, following Eq. S4	39.7	-2.48	160.4	39.2	0.00	20
GFDL-AM2.1, subtropical on	Imposed between 15° and 30°, following Eq. S5	39.7	1.29	160.4	-3.0	-0.52	20
GFDL-AM2.1, LW on	Only longwave cloud radiative effects imposed	39.7	-0.91	160.4	71.0	-6.78	30
GFDL-AM2.1, SW on	Only shortwave cloud radiative effects imposed	39.7	1.17	160.4	-16.9	-2.08	30
NCAR-CAM5.3, extratropical on	Imposed poleward of 30°, following Eq. S2	42.3	2.57	135.6	2.06	-3.73	5
NCAR-CAM5.3, tropical on	Imposed equatorward of 30°, following Eq. S3	42.3	-3.04	135.6	34.4	-1.04	5

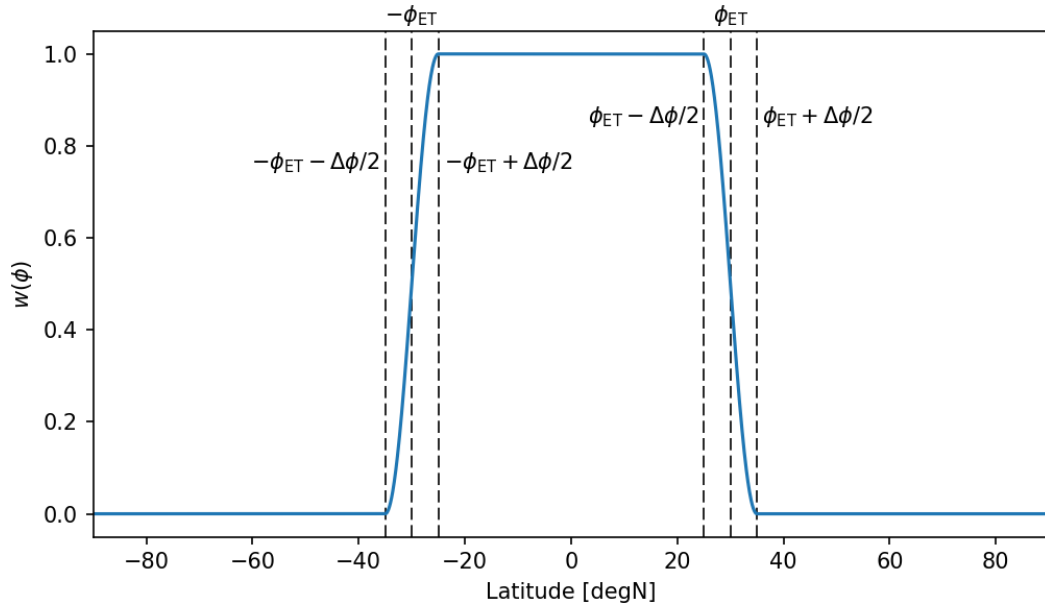
71

72

73

74 **Figures**

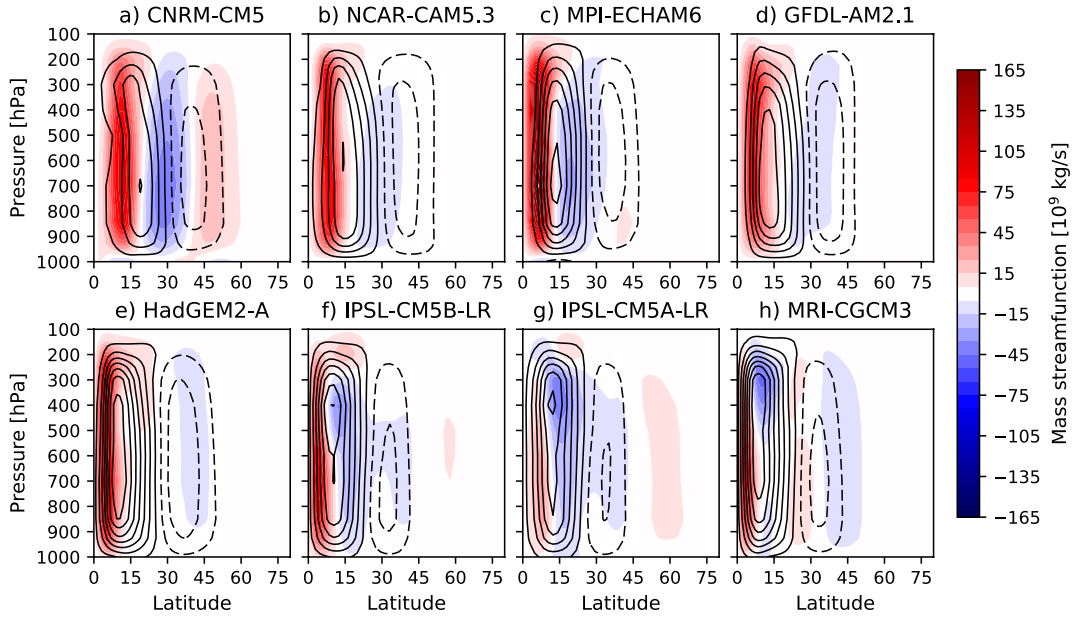
75



76

77 **Figure S1:** The weighting function  $w(\phi, \phi_{ET}, \Delta\phi)$  that is used to weight the total and clear-  
 78 sky radiative fluxes and heating rates in order to include cloud radiative effects in only  
 79 certain latitude bands. Here the weighting function is shown for the parameters  $\phi_{ET} = 30^\circ$   
 80 and  $\Delta\phi = 10^\circ$  (see Eq. S1).

81



82

83 **Figure S2:** The mass streamfunction in the clouds off experiment (black contours,  $30 \times 10^9$   
 84 kg/s intervals) and the difference in mass streamfunction between the clouds on and clouds  
 85 off experiment (shaded contours) for each model in the COOKIE ensemble. Positive (solid)  
 86 contours indicate a clockwise circulation and negative (dashed) contours indicate a  
 87 counter-clockwise circulation.

88

89

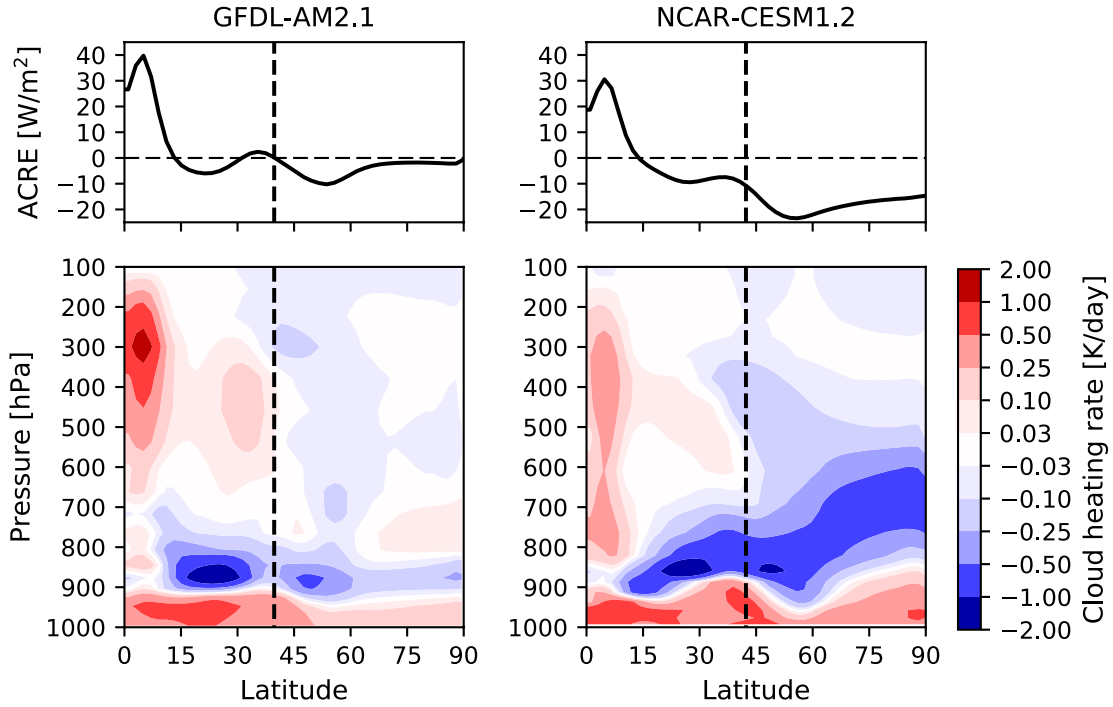
90

91

92

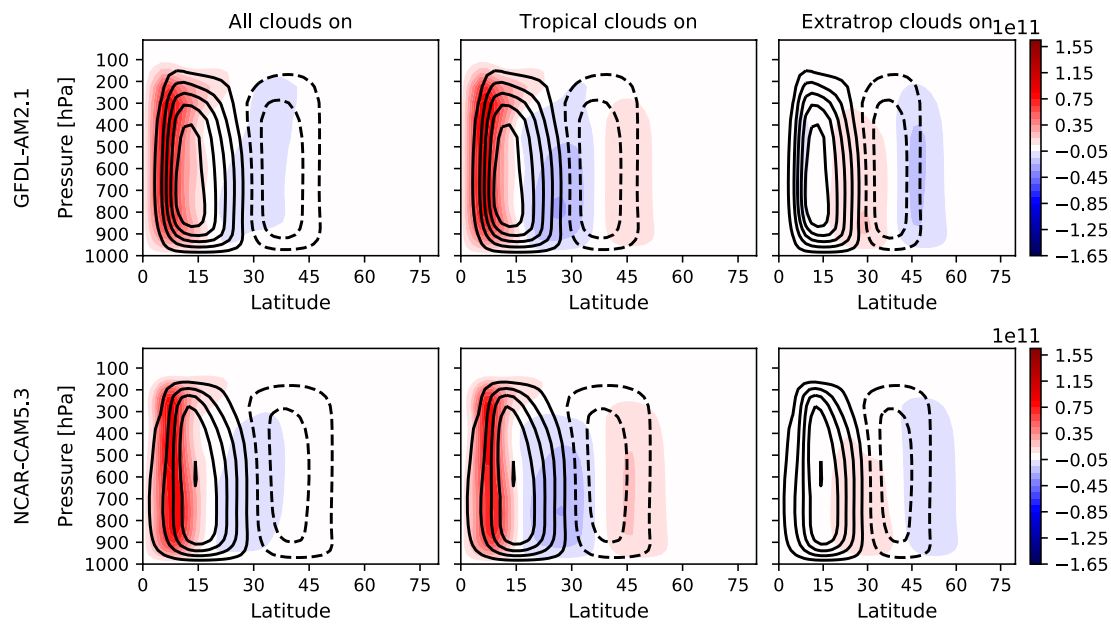
93

94



95  
96 **Figure S3:** The ACRE (top row) and cloud heating rate (bottom row) for the GFDL-AM2.1  
97 model (left column) and the NCAR-CESM1.2 model (right column), both for the clouds-on  
98 experiment. The cloud heating rate is taken as the difference between the total and clear-  
99 sky heating rates, summed over both the longwave and shortwave bands. The ACRE can be  
100 computed as the vertical integral of the cloud heating rate:  $\text{ACRE} = \frac{c_p}{g} \int_0^{p_s} Q_{\text{clu}}(\mathbf{p}) d\mathbf{p}$ . The  
101 vertical dashed lines mark the latitude of the eddy-driven in the clouds-off simulation ( $\phi_{\text{off}}$ ).  
102  
103  
104  
105  
106  
107

108



109

110 **Figure S4:** The mass streamfunction in the GFDL-AM2.1 (top row) and NCAR-CAM5.3  
111 (bottom row) clouds off experiment (black contours,  $30 \times 10^9$  kg/s intervals) and, in the  
112 difference in mass streamfunction ( $10 \times 10^9$  kg/s interval) between the (a) all  
113 clouds on, (b) tropical clouds on and (c) extratropical clouds on and clouds off experiments  
114 with the GFDL AM2.1 model. Positive (solid) contours indicate a clockwise circulation and  
115 negative (dashed) contours indicate a counter-clockwise circulation.

116

117

118

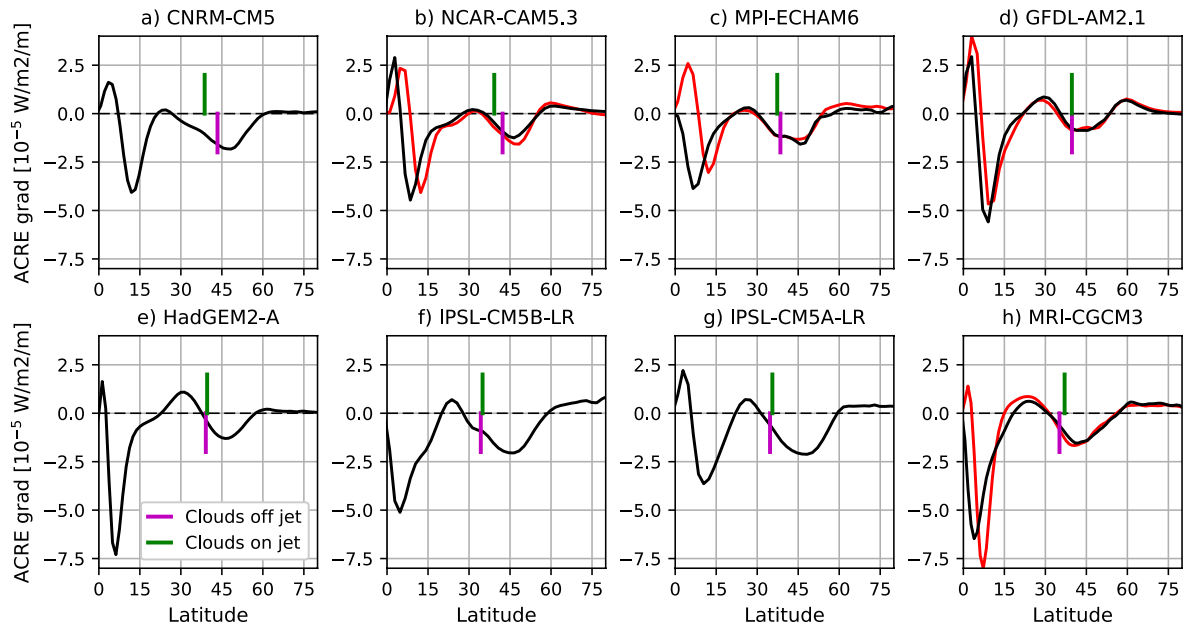
119

120

121

122

123



124

125 **Figure S5:** The meridional gradient of ACRE for the clouds-on simulations of each model  
126 (black) and the ACRE for the clouds-off simulation of each model, where available. The  
127 latitude of the eddy-driven jet in the clouds off and clouds on simulations marked by  
128 vertical magenta and green lines, respectively. In panel h), the height-dependent cloud  
129 heating rate for the GFDL-AM2.1 model.

130

131

132

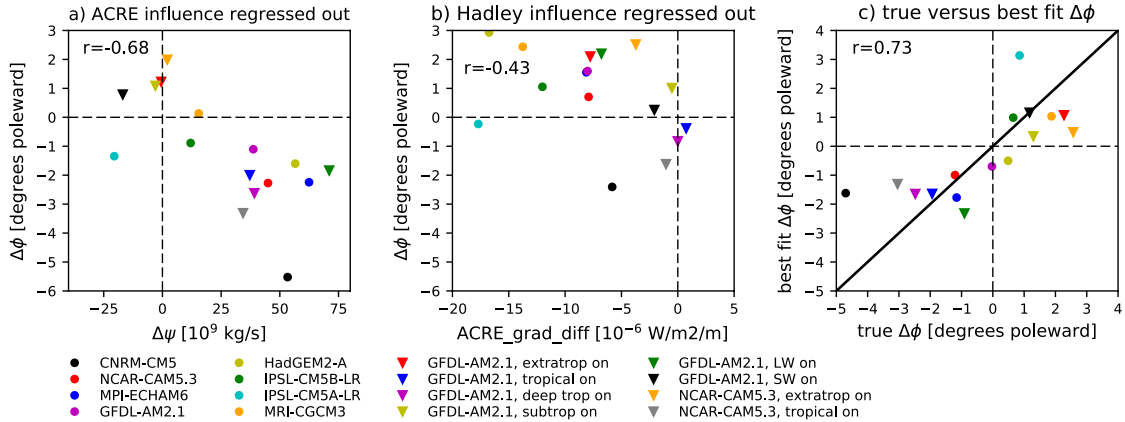
133

134

135

136

137



138

139 **Figure S6:** Scatter plots of a)  $\Delta\psi$  versus  $\Delta\phi$  after removing influence of  $\text{ACRE\_grad\_diff}$ , b)  
 140  $\text{ACRE\_GRAD\_diff}$  versus  $\Delta\phi$  after removing influence of  $\Delta\psi$ , (see text for details) and c) the  
 141 true  $\Delta\phi$  versus the best fit  $\Delta\phi$  computed using Eq. 3 for each experiment.

142

143

144